A Cu^{2+} ($S = {}^1\!/_2$) Kagomé Antiferromagnet: Mg$_x$Cu$_{4-x}$(OH)$_6$Cl$_2$

Shaoyan Chu,[†] Tyrel M. McQueen,[‡] Robin Chisnell,[§] Danna E. Freedman,[‡] Peter Müller,[‡] Young S. Lee,[§] and Daniel G. Nocera*,[‡]

Department of Chemistry, Department of Physics, and Center for Materials Science and Engineering, Massachusetts Institute of Technology, 77 Massachusetts Avenue, Cambridge, Massachusetts 02139

Received January 30, 2010; E-mail: nocera@mit.edu

Geometric frustration of magnetic ordering in triangle-based lattices is thought to be one avenue for inducing macroscopic quantum states in electron systems.[1] Because of the triangular arrangement of ions, it is impossible to satisfy all of the nearest-neighbor interactions simultaneously (Figure 1a). This "frustration" suppresses classical magnetic long-range order (LRO) and is thought to be capable of producing novel quantum states such as the resonating-valence-bond (RVB) or "spin-liquid" ground state for a two-dimensional (2D) $S = {}^1\!/_2$ antiferromagnet.[2] However, "structurally perfect" frustrated materials are rare; frequently, triangular lattices undergo a structural distortion at low temperature that relieves the magnetic frustration and gives rise to a classical ground state.[3−6] One of the few known examples is the $x = 1$ end member of the paratacamite series Zn$_x$Cu$_{4-x}$(OH)$_6$Cl$_2$.[7−10] It has a perfect 2D kagomé (corner-sharing triangle) lattice of Cu^{2+}($S = {}^1\!/_2$) ions in Jahn−Teller-distorted O$_4$Cl$_2$ octahedra separated by layers of Zn^{2+} in O$_6$ octahedra. However, the chemical similarity between Zn^{2+} and Cu^{2+} combined with the difficulty in differentiating Zn and Cu by X-ray and neutron diffraction techniques has complicated studies of this material, as site mixing of Zn and Cu in the kagomé planes may also account for the observed behaviors.[11] Herein we report the structural and magnetic characterization of a new series of compounds, Mg$_x$Cu$_{4-x}$(OH)$_6$Cl$_2$, that are isostructural with paratacamite.[12] Whereas both Mg and Cu can occupy the interplane O$_6$ site, the ligand-field chemistry of non-Jahn−Teller-active Mg strongly disfavors its residency within the tetragonally distorted O$_4$Cl$_2$ coordination sites in the kagomé plane. This disparity in the ligand-field chemistry of Mg and Cu ensures minimal substitution of Cu by Mg into the kagomé interlayer.

Synthesis of Mg$_x$Cu$_{4-x}$(OH)$_6$Cl$_2$ proceeded in a manner analogous to that for paratacamite.[8] In a typical reaction, Cu$_2$(OH)$_2$CO$_3$ and a large excess of MgCl$_2$·6H$_2$O (2−4 Mg per 1 Cu) were combined at 130−190 °C under hydrothermal conditions. After 2−3 days, a blue-green powder of Mg$_x$Cu$_{4-x}$(OH)$_6$Cl$_2$ formed at the base of the reaction vessel. The Mg content in the product was controllable, with higher Mg excesses and lower temperatures producing samples with larger x. Results for polycrystalline samples with $x = 0.39$ (**1**), 0.54 (**2**), and 0.75 (**3**) are reported here. Attempts to prepare samples with higher x were unsuccessful. Millimeter-sized crystals with $x = 0.33$ (**4**), 0.65 (**5**), and 0.75 (**6**) were grown under hydrothermal conditions in a temperature gradient from powders placed at the hot end (190 °C) of the reaction vessel. Blue-green, octahedral crystals formed at the cold end. Detailed synthesis procedures and crystallographic X-ray data can be found in the Supporting Information.

As shown in Figure 1b, the trigonal crystal structure of Mg$_x$Cu$_{4-x}$(OH)$_6$Cl$_2$ consists of 2D kagomé layers perpendicular to
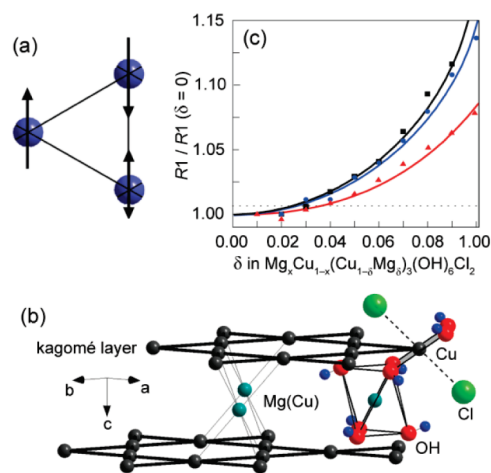
Figure 1. (a) The simplest geometric unit in which magnetic frustration can occur is a triangle. (b) Idealized structure of Mg$_x$Cu$_{4-x}$(OH)$_6$Cl$_2$, illustrating the 2D kagomé arrangement of Cu^{2+} ions separated by interlayer cations. (c) Plot of the X-ray refinement statistic $R1$ as a function of δ, the fraction of sites in the kagomé plane occupied by Mg for a fixed content x [Mg$_x$Cu$_{1-x}$(Cu$_{1-\delta}$Mg$_\delta$)$_3$(OH)$_6$Cl$_2$]: $x = 0.33$ (■, black), $x = 0.65$ (●, blue), $x = 0.75$ (▲, red). $R1$ is normalized to the value when $\delta = 0$; at most, only 3% of the in-plane Cu^{2+} atoms are replaced by nonmagnetic Mg^{2+}. The dashed line corresponds to the 95% confidence level for one extra parameter in the Hamilton R-ratio test. The lines are guides to the eye.

the c axis. These layers are built from corner-sharing CuO$_4$ plaquettes, which are tilted with respect to each layer. Triangles of the networks are bridged by MgO$_6$ octahedra between the layers separated by Cl$^-$ anions. Nominally, the in-plane, Jahn−Teller-distorted O$_4$Cl$_2$ sites are entirely occupied by Cu^{2+}, with Mg^{2+} being incorporated solely into the interplane O$_6$ site, and thus, the formula can logically be written as (Mg$_x$Cu$_{1-x}$)Cu$_3$(OH)$_6$Cl$_2$. To quantify the maximum amount of Mg at in-plane sites, several different tests were performed using the single-crystal data. First, refinements were performed assuming no mixing of Mg into the kagomé planes. Subsequently, the Mg/Cu ratio in the plane was allowed to vary, adding one additional parameter to the refinement. By the Hamilton R-ratio test,[13] including this one extra parameter was barely on the edge of statistical significance at the 95% confidence level (1.008, 1.008, and 1.008 for **4**, **5**, and **6**, respectively, versus a cutoff of 1.008). Furthermore, the freely refined Mg content in the kagomé planes was small in each case, at most 5.5 standard deviations away from zero [0.005(13), 0.032(9), and 0.047(9) for **4**, **5**, and **6**, respectively]. Thus, the amount of mixing, if any, was small. As a more robust quantification of the maximum amount of Mg at the in-plane sites, Figure 1c shows values of the X-ray refinement statistic $R1$ obtained from refinements of the single-crystal X-ray data for **4**, **5**, and **6** at 100 K at various fixed levels of Mg in the kagomé layers (normalized to the value obtained with no mixing). In each case, the minimum is sharp and consistent with at most
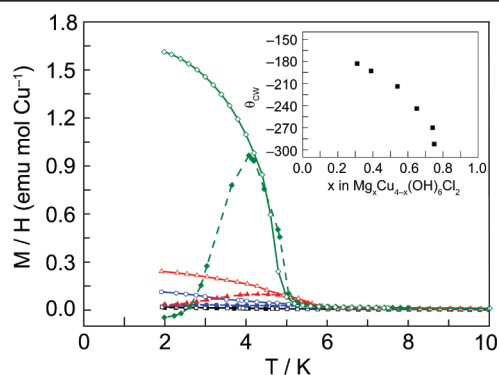
Figure 2. Field-cooled (open symbols) and zero-field-cooled (filled symbols) magnetization data ($H_{appl} = 200-500$ Oe) for $Mg_xCu_{4-x}(OH)_6Cl_2$ samples [$x = 0.75$ (□/■, black), $x = 0.54$ (○/●, blue), $x = 0.39$ (△/▲, red), $x = 0.33$ (◇/◆, green)]. Inset: Curie−Weiss temperatures for samples with varying x extracted from fits of the high-temperature magnetic susceptibility.

3% of the Cu^{2+} being replaced by Mg^{2+}. This is significantly less than the $7-10\%$[11] that has been proposed for $Zn_xCu_{4-x}(OH)_6Cl_2$ on the basis of neutron diffraction data and confirms that, at least in $Mg_xCu_{4-x}(OH)_6Cl_2$, the observed magnetic behavior cannot be due to significant disorder within the 2D kagomé planes.

Field-cooled (FC) and zero-field-cooled (ZFC) magnetization data were collected for samples **1−4** [$Mg_xCu_{4-x}(OH)_6Cl_2$, $x = 0.39, 0.54, 0.75, 0.33$] at $2-10$ K under applied dc fields of $200-500$ Oe (Figure 2). For all of the samples, the estimated susceptibility, M/H, was small from room temperature down to $5-6$ K. Below $5-6$ K, M/H increased sharply, indicative of ferromagnetic-like magnetic ordering (likely canted antiferromagnetism). Although the magnitude of the transition at ~5 K changed significantly with composition, the temperature at which the transition occurred was essentially composition independent (Figure S6 in the Supporting Information). With increasing substitution of Mg at the interlayer site, the maximum value of the susceptibility decreased, with a corresponding decrease in the splitting between the FC and ZFC data. By $x = 0.75$, only a faint upturn remained.

The suppression of ordering with increasing x can be explained if the ferromagnetic-like behavior arises from magnetic coupling between the kagomé layer Cu^{2+} and the interlayer Cu^{2+} ions. When x is small, there is significant coupling between neighboring kagomé layers, giving rise to regions of magnetic order, as is observed in the $x = 0$ end member, clinoatacamite.[14] As the number of interlayer Cu^{2+} ions decreases (with increasing x), there are fewer magnetic exchange pathways between layers. This leads to a progressive decrease in the size and number the magnetically ordered domains, which exist only where interlayer coupling is present. Consequently, as x increases, the sample displays a smaller ferromagnetic response. This model also explains why the temperature at which the upturn appears is composition-independent. While the number of interlayer Cu^{2+} ions affects the fraction of the sample exhibiting ferromagnetism, the intrinsic temperature at which ordering occurs it set by the magnitude of the coupling through a given interlayer Cu^{2+}. The size of this coupling is determined by the Cu−O bond lengths and Cu−O−Cu bond angles. The X-ray data show that the structural parameters depend only weakly on composition (Figure S4), and thus, the temperature at which ferromagnetism appears should be only weakly x-dependent.

Interlayer Cu^{2+} magnetic coupling is further supported by the change in the Curie−Weiss temperature (θ_{CW}), which is a measure of the strength of the magnetic interactions, across the series. The Curie−Weiss constants for these samples were extracted from fits

of the high-temperature inverse susceptibility data (Figure S5). The inset of Figure 2 shows θ_{CW} as a function of x. The values are large and negative, indicating strong antiferromagnetic exchange. The degree of magnetic frustration can be ascertained from the ratio of the ordering temperature to the Curie−Weiss constant [here $|\theta_{CW}|/T_N \geq 30$, with a minimum cutoff of 10 taken to mean strong frustration]. As x varies from 0.33 to 0.75, θ_{CW} becomes more negative by nearly a factor of 2, suggesting a strong increase in antiferromagnetic interaction and magnetic frustration. Inasmuch as the actual geometry is unchanged over the entire series [e.g., the in-plane Cu−O−Cu angle is 119.12(12)° for $x = 0.33$ and 119.06(9)° for $x = 0.75$], the strength of magnetic coupling within the planes is constant. Thus, the interactions between in-plane and interplane sites due to Cu^{2+} in the O_6 octahedra are ferromagnetic and give rise to the magnetic order observed. These data also suggest that as x approaches unity, no magnetic transition should remain, despite only a small maximum amount of Mg/Cu site disorder. The absence of magnetic disorder, which is similar to that observed in $Zn_xCu_{4-x}(OH)_6Cl_2$,[8] is consistent with an exotic ground state in these materials.

Interlayer Cu^{2+} atoms in $Mg_xCu_{4-x}(OH)_6Cl_2$ exhibit ferromagnetic coupling to in-plane, kagomé Cu^{2+} ions. However, magnetic ordering is suppressed when Cu^{2+} ions are absent from the interlayer. Within the kagomé layers, minimal substitution of Mg^{2+} for Cu^{2+} ($\leq 3\%$) is observed because of the significantly different ligand-field chemistry of these two ions. The absence of magnetic order and minimal site disorder within the kagomé planes suggests an unconventional magnetic ground state for $Mg_xCu_{4-x}(OH)_6Cl_2$. These results imply that the lack of a magnetic-ordering transition in materials with this structure type, such as $ZnCu_3(OH)_6Cl_2$, which also does not become magnetically ordered even at temperatures as low as 50 mK,[10,11] is not due to chemical disorder but is indeed a result of the high spin frustration within the kagomé planes.

Supporting Information Available: Complete synthetic protocols, Curie−Weiss fits of magnetic susceptibilities, and X-ray diffraction results (CIF). This material is available free of charge via the Internet at http://pubs.acs.org.

References

(1) Moessner, R.; Ramirez, A. R. *Phys. Today* **2006**, *59*, 24–29.
(2) Anderson, P. W. *Mater. Res. Bull.* **1973**, *8*, 153–160.
(3) Greedan, J. E. *J. Mater. Chem.* **2001**, *11*, 37–53.
(4) Ramirez, A. P. *Annu. Rev. Mater. Sci.* **1994**, *24*, 453–480.
(5) McQueen, T. M.; Stephens, P. W.; Huang, Q.; Klimczuk, T.; Ronning, F.; Cava, R. J. *Phys. Rev. Lett.* **2008**, *101*, 166402.
(6) Collins, M. F.; Petrenko, O. A. *Can. J. Phys.* **1997**, *75*, 605–655.
(7) Braithwaite, R. S. W.; Mereiter, K.; Paar, W. H.; Clark, A. M. *Min. Mag.* **2004**, *68*, 527–539.
(8) Shores, M. P.; Nytko, E. A.; Bartlett, B. M.; Nocera, D. G. *J. Am. Chem. Soc.* **2005**, *127*, 13462–13463.
(9) Lee, S. H.; Kikuchi, H.; Qiu, Y.; Lake, B.; Huang, Q.; Habicht, K.; Kiefer, K. *Nat. Mater.* **2007**, *6*, 853–857.
(10) Helton, J. S.; Matan, K.; Shores, M. P.; Nytko, E. A.; Bartlett, B. M.; Yoshida, Y.; Takano, Y.; Suslov, A.; Qiu, Y.; Chung, J. H.; Nocera, D. G.; Lee, Y. S. *Phys. Rev. Lett.* **2007**, *98*, 107204.
(11) de Vries, M. A.; Kamenev, K. V.; Kockelmann, W. A.; Sanchez-Benitez, J.; Harrison, A. *Phys. Rev. Lett.* **2008**, *100*, 157205.
(12) The mineral haydeeite has a similar formula, $MgCu_3(OH)_6Cl_2$, but a different structure than the compounds reported here.
(13) Hamilton, W. C. *Acta Crystallogr.* **1965**, *18*, 502.
(14) Zheng, X. G.; Kawae, T.; Kashitani, Y.; Li, C. S.; Tateiwa, N.; Takeda, K.; Yamada, H.; Xu, C. N.; Ren, Y. *Phys. Rev. B* **2005**, *71*, 052409.

JA1008322